

Molecular Dynamic Simulation and Receptor-based Pharmacophore Modeling on Human Renin for Discovery of Novel Inhibitors

Chanin Park, SundarapandianThangapandian, Yuno Lee, Minky Son, Shalini John, Young-sik Sohn, and Keun Woo Lee

Abstract—Hypertension is characterized with stress on the heart and blood vessels thus increasing the risk of heart attack and renal diseases. The Renin angiotensin system (RAS) plays a major role in blood pressure control. Renin is the enzyme that controls the RAS at the rate-limiting step. Our aim is to develop new drug-like leads which can inhibit renin and thereby emerge as therapeutics for hypertension. To achieve this, molecular dynamics (MD) simulation and receptor-based pharmacophore modeling were implemented, and three rennin-inhibitor complex structures were selected based on IC₅₀ value and scaffolds of inhibitors. Three pharmacophore models were generated considering conformations induced by inhibitor. The compounds mapped to these models were selected and subjected to drug-like screening. The identified hits were docked into the active site of renin. Finally, hit1 satisfying the binding mode and interaction energy was selected as possible lead candidate to be used in novel renin inhibitors.

Keywords—Renin inhibitor, Molecular dynamics simulation, Structure-based pharmacophore modeling.

I. INTRODUCTION

HYPERTENSION is a major cardiovascular risk factor associated with significant morbidity and mortality worldwide [1]. It remains poorly controlled in many patients and often requires combination therapy to achieve the targeted blood pressure lowering. The renin-angiotensin system (RAS) is an important regulator of salt and water homeostasis and has a key role in the control of blood pressure (Fig. 1). The RAS is stimulated by a number of signals, including a drop in blood

Chanin Park is with the Division of Applied Life Science (BK21 program), Gyeongsang National University (GNU), 501 Jinju-daero, Gazwa-dong, Jinju 660-701, Republic of Korea (phone: +82-55-772-1360; fax: +82-55-772-1359; e-mail: chip@bio.gnu.ac.kr).

SundarapandianThangapandian is with the Division of Applied Life Science, Gyeongsang National University (GNU), 501 Jinju-daero, Gazwa-dong, Jinju 660-701, Republic of Korea (e-mail: sunder@bio.gnu.ac.kr).

Yuno Lee is with the Division of Applied Life Science (BK21 program), Gyeongsang National University (GNU), 501 Jinju-daero, Gazwa-dong, Jinju 660-701, Republic of Korea (e-mail: yuno@bio.gnu.ac.kr).

Minky Son is with the Division of Applied Life Science (BK21 program), Gyeongsang National University (GNU), 501 Jinju-daero, Gazwa-dong, Jinju 660-701, Republic of Korea (e-mail: minky@bio.gnu.ac.kr).

Shalini John is with the Division of Applied Life Science, Gyeongsang National University (GNU), 501 Jinju-daero, Gazwa-dong, Jinju 660-701, Republic of Korea (e-mail: shalini@bio.gnu.ac.kr).

Young-sik Sohn is with the Division of Applied Life Science, Gyeongsang National University (GNU), 501 Jinju-daero, Gazwa-dong, Jinju 660-701, Republic of Korea (e-mail: ysohn@bio.gnu.ac.kr).

Keun Woo Lee is with the Division of Applied Life Science (BK21 program), Gyeongsang National University (GNU), 501 Jinju-daero, Gazwa-dong, Jinju 660-701, Republic of Korea (phone: +82-55-772-1360; fax: +82-55-772-1359; e-mail: kwlee@bio.gnu.ac.kr).

pressure, a decrease in circulating volume, or a reduction in plasma sodium concentration. Inhibition of the RAS is an effective way to intervene in the pathogenesis of cardiovascular and renal disorders [2]. The renin cleaves angiotensinogen to form the hemodynamically inactive decapeptide angiotensin I. The active octapeptide angiotensin II is converted from angiotensin I by the angiotensin-converting enzyme (ACE). The binding of angiotensin II to the type-1 angiotensin II receptors (AT1) triggers a number of physiological effects, ultimately leading to an increase in blood pressure [3]. Since renin controls the first rate-limiting step in the RAS cascade, renin inhibition is considered to be an attractive antihypertensive strategy [4]-[5].

The human renin, a 340-amino acid, is a member of the aspartyl protease superfamily [6]. Structurally, renin consists of 2 lobes with a long and deep cleft between them [7]-[8]. The cleft, the active site of renin, accommodates a 7-amino acid residue of angiotensinogen. Two aspartic acid residues (Asp38 and Asp226 in human renin), each located in a single lobe of renin, control the first and rate-limiting step of the RAS by catalyzing the hydrolysis of the Leu10-Val11 peptide bond of angiotensinogen and releasing the decapeptide Angiotensin I [9].

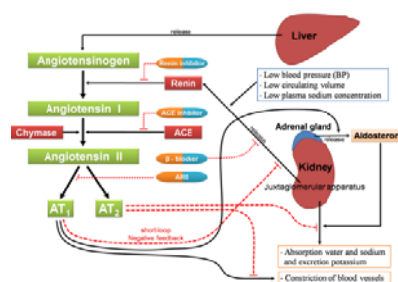


Fig. 1 The Renin Angiotensin System (RAS) and the sites of blockade. Renin is the rate-limiting step in the RAS cascade

Renin inhibitors have been predicted to be more efficacious with fewer side effects than ACE inhibitors and AT1 receptor antagonists [10]. The design and development of renin inhibitor have started with peptide mimicking the features of its only substrate angiotensinogen. These peptide based renin inhibitors followed by various synthetic peptides were not successful in treating hypertension as renin inhibitors [8], [11]-[13]. As none of these compounds survived the stages of drug development, there was a need for new classes of nonpeptide renin inhibitors that fulfill all criteria for becoming successful drugs [8].

Among the various efforts taken to develop renin inhibitors with good bioavailability, only aliskiren arose from the former peptidomimetic structures as a successful candidate. Aliskiren is the only renin inhibitor launched in the market as anti-hypertensive agent [14].

In this study, three receptor-based pharmacophore models were developed to consider the conformational diversity of the active site depending on bound. The MD simulations in general consider the conformational dynamics of protein by generating an ensemble of protein conformations. Developing a pharmacophore model taking into account the conformational changes in the active site is rational and will increase the reliability of the models [16]. These pharmacophore models were used in database screening to identify new and potential hits for future drug design. Molecular docking study has reduced the probability of picking false positives as potential hits. This methodology will be useful in identifying new renin inhibitors with similar binding orientation as existing compounds.

II. METHODS

A. Preparation of Systems

Among dozens of x-ray crystal structures of human renin-inhibitor complexes available in the protein data bank (PDB), three complex structures (PDB ID: 3G6Z [15], 3GW5 [17], and 2V0Z [8]) were selected based on the IC_{50} value (< 1.0 nM) and chemical scaffolds of bound inhibitors. These selected crystal structures have contained missing region at Glu167-Gln170, Leu1-Leu3, and Asn168, respectively. The complete structures that were repaired the missing region were prepared through the Build Homology Models protocol within Discovery Studio (DS) 2.5.

B. Molecular Dynamics Simulation

The MD simulations of three renin-inhibitor complex structures were performed with GROMOS96 force field using GROMACS 4.0.7 package [18]. Initially, all the ionizable residues in the protein were protonated at pH7. The topologies and charges for each inhibitor were calculated using the PRODRG web-server [19]. Each complex was solvated with the SPC water molecules. Eight Na^+ counter-ions were added to ensure the overall charge neutrality of the system. Energy minimization was performed with steepest descent algorithm. Then the protein was restrained and the solvent molecules with counter-ions were allowed to move during a 100 ps position-restrained MD run. The well equilibrated structure was then used for 5 ns production runs. The electrostatic contributions were calculated using the particle-mesh Ewald (PME) algorithm [20] with a direct interaction cut-off of 0.9 nm and grid spacing of 0.12 nm. The van der Waals (VDW) forces were treated by using a cut-off of 1.4 nm. All simulations were executed under periodic boundary conditions with the NPT ensemble using the V-rescale thermostat and Parrinello-Rahman barostat for keeping the temperature (300 K) and the pressure (1 bar) constant. Bonds between heavy atoms and corresponding hydrogen atoms were constrained to their equilibrium bond lengths using the LINCS algorithm [21] and

the geometry of water molecules was constrained using the SETTLE algorithm [22]. The time step for the simulation was 2 fs and the coordinates were stored every 1 ps.

C. Cluster Analysis

Selection of a representative structure which could represent the conformational flexibility of the protein throughout the simulation time is crucial. Therefore, three representative structures were selected from each simulation trajectory of 5000 frames saved during the simulation time. The `g_cluster` implemented in GROMACS was used for cluster analysis of the trajectories from 2001 ps to 5000 ps. From the RMSD comparisons of each snapshot with all the others, clusters were generated with the cut-off values of 0.143 nm (3G6Z), 0.128 nm (3GW5), and 0.120 nm (2V0Z) using `gromos` method.

D. Receptor-Based Pharmacophore Model Generation

The three representative structures obtained from the most populated clusters were used to generate receptor-based pharmacophore models screening the complementary pharmacophoric features in the active site of protein. The Interaction Generation protocol in DS was used to extract all the available hydrophilic and hydrophobic interaction points that can be complemented by the bound inhibitor. The representative features including hydrogen bond acceptor (HBA), hydrogen bond donor (HBD), and hydrophobic (HYP) features were selected based on the active site residues. The final pharmacophore model consists of the essential pharmacophoric features, which are supposed to be present in the inhibitor.

E. Database Screening and Drug-Like Filtration

The three receptor-based pharmacophore models were used as 3D structural queries in database screening in order to find potential hit compounds suitable for further progress. The screening calculation was carried out using the Ligand Pharmacophore Mapping protocol with the Best/Flexible search option in DS. Two chemical databases containing diverse chemical compounds were used in database screening. The fit value for filtering hit compounds was set based on the fit values of already known renin inhibitors. Hit compounds with higher fit value than any of the fit value of known most active compounds were selected and checked for their drug-like properties using Lipinski's rule of five and ADMET filters using DS. Final hit compounds that passed all of these screening tests were selected and used in molecular docking study.

F. Molecular Docking and Interaction Energy

Molecular docking studies for final hit compounds were performed using GOLD 4.1 program [23]. The active sites of three representative structures were defined with a radius of 10 Å around the bound inhibitor. All hit compounds from database screening along with the bound inhibitors in three crystal structures were docked into the active site. The Maximum save conformations was set to 10 and the Early Termination was set as 5 to skip the calculation if the RMSD between any of the 5 docked conformations is less than 1.5 Å. Energy minimization

calculations were performed to refine top 5 docked structures for three systems using DS. The Smart Minimizer algorithm was used to relax the docked conformations and remove steric overlaps that produce bad contacts between docked compounds and protein. The parameters for energy minimization used 5,000 max steps, RMS Gradient of 0.1 kcal/mol, and the Distance-Dependent Dielectrics for implicit solvent model. Interaction energies for all minimized structures were measured using the Calculate Interaction Energy protocol with the Implicit Distance-Dependent Dielectrics model option in DS.

III. RESULTS

A. Selection and Preparation of Structures

Three renin-inhibitor complex structures were selected to consider the conformational diversity of the active site depending on the bound inhibitors (Table I). For three structures 3G6Z, 3GW5, and 2V0Z, the IC₅₀ values of bound compounds were 0.16nM, 0.4nM, and 0.6nM as the most active inhibitors, respectively. These bound compounds are of structurally diverse scaffolds to each other. The A7T (Inh1) of 3G6Z contains a fused ring system with other substitutions, whereas the 72X (Inh2) of 3GW5 is a piperidine derivative. The C41 (Inh3) of 2V0Z is aliskiren, the first marketed renin inhibitor, which contains only one substituted phenyl ring with long substitutions. These three structures reflect the conformational diversity of active site of renin that can accommodate diverse chemical compounds. These three x-ray structures with recovered missing regions, corrected bond orders, and added hydrogens were taken as initial structures for MD simulation studies.

TABLE I

LIST OF CRYSTAL STRUCTURES OF RENIN WITH DIFFERENT INHIBITORS

PDB ID	Resolution (Å)	Inhibitor	IC ₅₀ (nM)
3G6Z	2.00	A7T (Inh1)	0.16
3GW5	2.00	72X (Inh2)	0.47
2V0Z	2.20	C41 (Inh3)	0.6

B. Stability of Simulations

Three MD simulations of Renin-Inh1, Renin-Inh2, and Renin-Inh3 complex structures were performed to construct refined and adjusted structures used to generate the receptor-based pharmacophore models. The stabilities of the three simulations were examined by calculating the root-mean-square deviation (RMSD), potential energy, and the number of intra-protein hydrogen bonds.

The RMSD values of the protein Cα atoms for three systems were measured with respect to their initial configurations, as a function of the simulation time (Fig. 2a). The stabilities of the simulations were achieved in the atom positional RMSD with values between 0.15 nm and 0.3 nm. During the first 600 ps of the simulation, the RMSD values of Renin-Inh1 and Renin-Inh3 systems increased up to ~ 0.17 nm and ~ 0.2 nm, respectively. After this time, the values of RMSD were

maintained until the end of the simulation time. On the other hand, the RMSD value of Renin-Inh2 was continued to gradually increase up to ~ 0.28 nm and kept a stable level after 2000 ps. From the RMSD analysis of the MD simulations, we can conclude that the three systems were stable in the simulation environment during the simulation time.

The calculations of potential energies and the number of intra-protein hydrogen bonds of the systems were also carried out to confirm the stabilities of the simulations. The potential energy of each system was maintained at about - 833828 kJ/mol (Renin-Inh1), - 760559 kJ/mol (Renin-Inh2), and - 798930 kJ/mol (Renin-Inh3), which indicates that the simulations are energetically stable (Fig. 2b). In addition, all the systems were kept about 225 intra-protein hydrogen bonds for the period of the simulation (Fig. 2c). These results show that there are no abnormal conformational changes in the proteins throughout the simulation. Although the number of intra-protein hydrogen bonds was similar, potential energies differ in each system. These differences appear to result from diverse interaction pattern between active site residues and bound inhibitors. In conclusion, these analyses have revealed that all three systems were stable during the simulation time and thus confirmed their reliability with no artifacts.

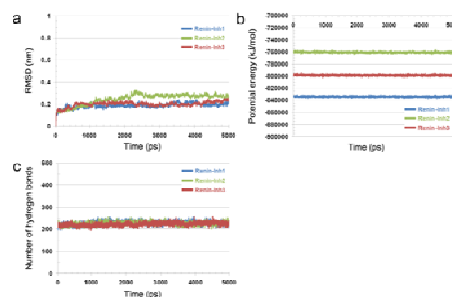


Fig. 2 Results of simulation stability analyses for three systems. a Cα RMSD with respect to the initial structure, b the potential energy, and c the number of intra-protein hydrogen bonds are plotted throughout the 5 ns MD simulation

C. Selection of Representative Structures

In order to select the representative structures to generate receptor-based pharmacophore models, cluster analyses were performed using the snapshots obtained from last 3000 ps (Fig. 3). The conformational families were statistically classified by comparing the active site conformations of the 3000 snapshots. In Renin-Inh1 and Renin-Inh3, totally eight clusters were characterized and the top clusters were composed of 71.83 % (2155 snapshots) and 61.47 % (1844 snapshots) of the total conformations, respectively. In case of Renin-Inh2, the top cluster among nine clusters was comprised of 55.83 % (1675 snapshots) of the total conformations. The 3667 ps (Rep1), 3961 ps (Rep2), and 3878 ps (Rep3) snapshots that are middle structures of each top cluster were selected as representative structures of Renin-Inh1, Renin-Inh2, and Renin-Inh3, respectively. These structures would be appropriate to represent the dynamic conformational space of the active site. All three representative structures were utilized in the development of pharmacophore models complementing the active site of the

protein.

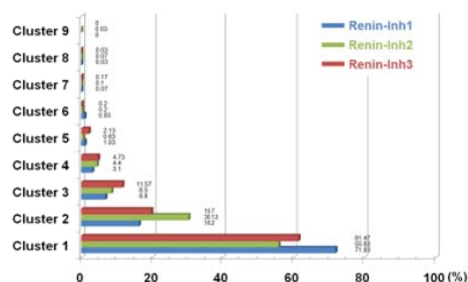


Fig. 3 The histogram obtained from the cluster analyses of last 3 ns of the 5 ns simulation

To investigate the conserved interacting residues in all three systems, comparison of three representative structures was carried out through analyzing the interaction patterns of three inhibitors with the active site residues (Fig. 4).

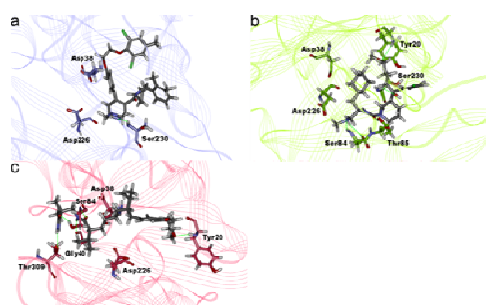


Fig. 4 Binding mode of each inhibitor in three representative structures. Binding conformations of a Inh1, b Inh2, and c Inh3 are compared along with hydrogen bond interacting residues. Rep1, Rep2, and Rep3 are colored in blue, green, and red, respectively. The inhibitors and residues are shown in stick model. Hydrogen bond interactions are represented by green dotted line

TABLE II
 CONSERVED RESIDUES INVOLVED IN INTERACTIONS

Interactions	Rep1	Rep2	Rep3
Hydrogen bond interaction	Ser230	Tyr20, Ser84, Thr85, Ser230	Tyr20, Ser84, Thr309
Hydrophobic interaction	Gln19, Val36, Trp45, Tyr83, Pro118, Phe119, Leu121, Ala122, Phe124, Val127, Ala229		

In Rep1, only one hydrogen bond interaction was formed between Inh1 and Ser230 (Fig. 4a). In case of Rep2, each residue, Tyr20, Thr85, and Ser230, has interacted with Inh2 through hydrogen bonding (Fig. 4b). Two hydrogen bond interactions were observed between Inh2 and Ser84. In Rep3, Inh3 has formed a hydrogen bond interaction with each residue, Tyr20, Gly40, and Thr309 (Fig. 4c). There were two hydrogen bond interactions between Inh3 and Ser84. Although there is no hydrogen bond interacting residue conserved in all three systems, Tyr20 and Ser84 were found to be involved in hydrogen bonding in both Rep2 and Rep3, and Ser230 in both

Rep1 and Rep2 (Table II). In addition, total 11 hydrophobic interacting residues conserved in all three systems were also observed. From the comparison of three representative structures, key hydrogen bond and hydrophobic interacting residues were identified and then considered to generate pharmacophore models.

D. Receptor-Based Pharmacophore Model Generation

Three receptor-based pharmacophore models were built using the representative structures obtained from the cluster analyses. The HBA, HBD and HYP chemical features were generated based on the consideration of the direction of each feature, but specific features were chosen depending on the direction in which each inhibitor formed interactions with the active site residues of renin (Fig. 5).

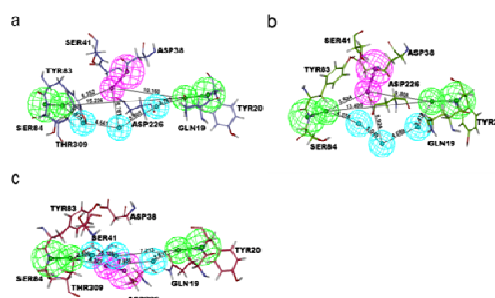


Fig. 5 The receptor-based pharmacophore models generated from three representative structures. 3D pharmacophore features of a Pharm1, b Pharm2, and c Pharm3 with inter-feature distance constraints are complemented hydrogen bond interacting residues. HBA, HBD, and HYP features are shown in green, magenta, and cyan, respectively. Residues of Rep1, Rep2, and Rep3 are colored in blue, green, and red, respectively, and shown in stick model

Six pharmacophoric features containing two HBA, one HBD, and three HYP were selected as a pharmacophore model (Pharm1) from Rep1. Two HBA features of Pharm1 were generated as complementary features to the main chain of Ser84 and Tyr20. A HBD feature was generated as a complimentary feature to the carboxyl group of Asp38. The Tyr20 and Ser84 involve in the hydrogen bond interaction with inhibitor during the simulation. The three HYP features were generated to hydrophobically interact with the active site residues and worked as the proper connecting points for HBA and HBD features (Fig. 5a). In addition to Pharm1, two more pharmacophore models, Pharm2 and Pharm3, were developed using Rep2 and Rep3, respectively. Similar to the generation of Pharm1, the pharmacophoric features of Pharm2 and Pharm3 were also created complementary to the important active site components (Fig. 5b, c). These two pharmacophore models were also made of two HBA, one HBD, and three HYP features. The HBA and HYP features of Pharm2 and Pharm3 were chosen based on the same residues as in Pharm1, but in Pharm3, the HBD feature was selected as a complimentary feature to the carboxyl group of Asp226 instead of Asp38. Because the carboxyl group of Asp38 moved aside from the active site during simulation time. Comparison of these three pharmacophore models revealed that each model contains same

pharmacophoric features but differs in terms of inter-feature distance constraints that explain the induced conformational changes upon inhibitor binding.

E. Database Screening and Drug-Like Filtration

The three developed pharmacophore models were utilized as 3D structural queries to retrieve potential drug candidates as a new renin inhibitor from two chemical databases namely Asinex and Maybridge. Chemical compounds mapped well on to the pharmacophoric features were retained and verified for their drug-like properties using Lipinski's rule of five and ADMET filters. Detailed description on the number of compounds retrieved from each step of database screening was shown in Fig. 6.

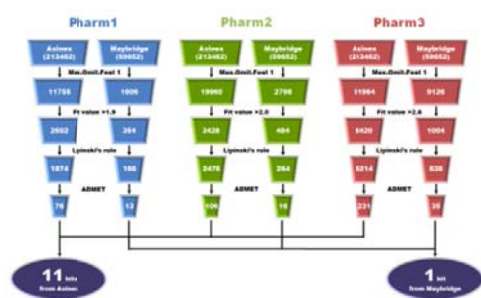


Fig. 6 Database screening result using three receptor-based pharmacophore models

From Asinex database, 76, 106, and 231 compounds were retrieved through Pharm1, Pharm2, and Pharm3, respectively. Finally, 11 compounds that are commonly passed through all three pharmacophore models were selected as hit compounds. On the other hand, 1 compound was chosen as hit compound from Maybridge database. Finally, a total of 12 hit compounds were obtained from the database screening process and considered for molecular docking study.

F. Molecular Docking and Interaction Energy

The molecular docking calculations were carried out to assess the 12 hit compounds obtained from database screening process and to investigate their binding orientation at the active site of renin. From the docking results, 5 hit compounds were selected based on the high GOLD fitness scores, proper binding orientations, and matching with their pharmacophore mapping. Three representative structures with each hit compound were subjected to the energy minimization to optimize their binding conformation of the hit compounds. Then, the interaction energies between each hit compound and renin were calculated and compared with that of the original three inhibitors (Table III).

TABLE III
INTERACTION ENERGIES (KCAL/MOL)

Inhibitors and Hits	Rep1	Rep2	Rep3
Inh1, Inh2, and Inh3	- 57.62554	- 16.32652	- 43.92793
Hit1	- 81.93515	- 84.64655	- 93.78731
Hit2	- 78.32083	- 88.52919	- 80.61787
Hit3	- 73.46501	- 75.72594	- 91.95759
Hit4	- 65.66974	- 69.28336	- 74.01645
Hit5	- 58.17558	- 66.85897	- 68.53240

The interaction energies of Inh1, Inh2, and Inh3 with renin were - 57.62554, - 16.32652, and - 43.92793 kcal/mol, respectively. All the 5 hit compounds of considerable chemical diversity (Fig. 7) were of lower interaction energy values than the three original inhibitors, but hit1 showing the lowest interaction energy and reasonable binding mode was only selected as final hit compound and candidate of potential antihypertensive agent.

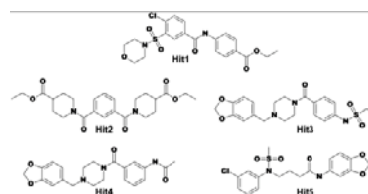


Fig. 7 Two-dimensional chemical structures of the hits filtered based on their GOLD fitness score and binding orientation

The mapping of this hit compound over all three pharmacophore models has revealed that this hit compound has mapped over all the features except for HBD in Pharm1 and Pharm2 and HBA in Pharm3 (Fig. 8).

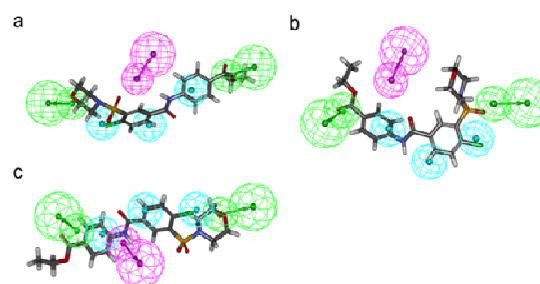


Fig. 8 Pharmacophore mapping. Hit1 is mapped on a Pharm1, b Pharm2, and c Pharm3. HBA, HBD, and HYP features are shown in green, magenta, and cyan, respectively

The binding orientations of the hit1 for Rep2 and Rep3 but not Rep1 were similar to each other and shown to have interaction with the active site residues complementing the pharmacophoric features. In Rep1, all 5 hit compounds were bound toward large hydrophobic cavity in the active site cleft that is formed by interaction of phenyl moiety with two chlorides of Inh1 with the active site residues. Consequently, their binding modes were not consistent with an orientation of

Pharm1. This result is because the active site conformation of Rep1 was optimized for Inh1. In Rep2 and Rep3, the binding modes of hit1 were similar to each other and to that of Inh3 (Fig. 9).

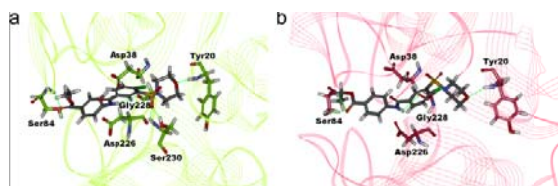


Fig. 9 Docking conformations of hit1 compound in two representative structures. Binding conformations of hit1 in a Rep2 and b Rep3 are compared along with hydrogen bond interacting residues. Rep2 and Rep3 are colored in green and red, respectively

Two phenyl rings of hit1 were mainly involved in the hydrophobic interactions. The hit1 has formed hydrogen bond interaction with hydrogen atom of backbone nitrogen of Tyr20 through oxygen atom of morpholine moiety. Two hydrogen bond interactions were found between oxygen atom of ethyl benzoate moiety of hit1 and two hydrogen atoms of backbone nitrogen and side chain oxygen of Ser84. There is a hydrogen bond interaction between hydrogen atom of amide moiety of hit1 and backbone oxygen atom of Gly228. Two hydrogen bond interactions between oxygen atom of sulfone moiety of hit1 and two hydrogen atoms of backbone nitrogen and side chain oxygen atom of Ser230 were only observed in Rep2, because the sulfone moiety was turned the opposite direction in Rep3. Although the number of hydrogen bonds between hit1 and the active site residues in Rep2 is more than that in Rep3, the interaction energy of - 93.78731 kcal/mol in Rep3 is lower than - 84.64655 kcal/mol in Rep2. This is caused by the difference in VDW interaction energies because the binding mode of the hit1 that is similar to Inh3 fit well the active site conformation optimized for Inh3. The VDW interaction energies of hit1 for Rep2 and Rep3 were - 35.1454 and - 53.1862 kcal/mol, respectively. Based on the combination of these results, we suggest that hit1 is of novel scaffold and potential virtual lead for renin inhibitor design.

ACKNOWLEDGMENT

This research was supported by Basic Science Research Program (2012R1A1A4A01013657), Pioneer Research Center Program (2009-0081539), and Management of Climate Change Program (2010-0029084) through the National Research Foundation of Korea (NRF) funded by the Ministry of Education, Science and Technology (MEST) of Republic of Korea. And this work was also supported by the Next-Generation BioGreen 21 Program (PJ008038) from Rural Development Administration (RDA) of Republic of Korea.

REFERENCES

[1] Murray CJL, Lopez AD, "Alternative projections of mortality and disability by cause 1990-2020: Global Burden of Disease Study," *The Lancet*, vol.349, no.9064, pp.1498-1504, 1997.

[2] Dzau V, "The cardiovascular continuum and renin-angiotensin-aldosterone system blockade," *Journal of hypertension*, vol. 23, S9, 2005.

[3] Kim S, Iwao H, "Molecular and cellular mechanisms of angiotensin II-mediated cardiovascular and renal diseases," *Pharmacological reviews*, vol. 52, no. 1, pp. 11, 2000.

[4] Cooper ME, "The role of the renin-angiotensin-aldosterone system in diabetes and its vascular complications," *American journal of hypertension*, vol. 17, pp. S16-S20, 2004.

[5] Norris K, Vaughn C, "The role of renin-angiotensin aldosterone system inhibition in chronic kidney disease," *Expert review of cardiovascular therapy*, vol. 1, no. 1, pp. 51-63, 2003.

[6] Wood JM, Stanton JL, Hofbauer KG, "Inhibitors of renin as potential therapeutic agents," *Journal of enzyme inhibition*, vol. 1, no. 3, pp. 169, 1987.

[7] Sielecki AR, Hayakawa K, Fujinaga M, Murphy M, Fraser M, Muir AK, Carilli CT, Lewicki JA, Baxter JD, James M, "Structure of recombinant human renin, a target for cardiovascular-active drugs, at 2.5 Å resolution," *Science*, vol. 243, no. 4896, pp. 1346, 1989.

[8] Rahuel J, Rasetti V, Maibaum J, Rueger H, Goschke R, Cohen N, Stutz S, Cumin F, Fuhrer W, "Structure-based drug design: the discovery of novel nonpeptide orally active inhibitors of human renin," *Chemistry & Biology*, vol. 7, no. 7, pp. 493-504, 2000.

[9] James MNG, Sielecki AR, "Stereochemical analysis of peptide bond hydrolysis catalyzed by the aspartic proteinase penicillopepsin," *Biochemistry*, vol. 24, no. 14, pp. 3701-3713, 1985.

[10] Stanton A, "Therapeutic potential of renin inhibitors in the management of cardiovascular disorders," *American Journal of Cardiovascular Drugs*, vol. 3, no. 6, pp. 389-394, 2003.

[11] Fisher NDL, Hollenberg NK, "Is there a future for renin inhibitors?," *Expert Opinion on Investigational Drugs*, vol. 10, no. 3, pp. 417-426, 2001.

[12] Wood JM, Maibaum J, Rahuel J, Grutter MG, Cohen NC, Rasetti V, Ruder H, Goschke R, Stutz S, Fuhrer W, "Structure-based design of aliskiren, a novel orally effective renin inhibitor," *Biochemical and biophysical research communications*, vol. 308, no. 4, pp. 698-705, 2003.

[13] Udenigwe CC, Li H, Aluko RE, "Quantitative structure-activity relationship modeling of renin-inhibiting dipeptides," *Amino Acids*, pp. 1-8, 2011.

[14] Claude Cohen N, "Structure-Based Drug Design and the Discovery of Aliskiren (Tekturna): Perseverance and Creativity to Overcome a RD Pipeline Challenge," *Chemical Biology & Drug Design*, vol. 70, no. 6, pp. 557-565, 2007.

[15] Bezenc on O, Bur D, Weller T, Richard-Bildstein S, Remen L, Sifferlen T, Corminboeuf O, Grisostomi C, Boss C, Prade L, "Design and Preparation of Potent, Nonpeptidic, Bioavailable Renin Inhibitors," *Journal of Medicinal Chemistry*, vol. 52, no. 12, pp. 3689-3702, 2009.

[16] Deng J, Lee KW, Sanchez T, Cui M, Neamati N, Briggs JM, "Dynamic receptor-based pharmacophore model development and its application in designing novel HIV-1 integrase inhibitors," *Journal of Medicinal Chemistry*, vol. 48, no. 5, pp. 1496-1505, 2005.

[17] Tice CM, Xu Z, Yuan J, Simpson RD, Cacatian ST, Flaherty PT, Zhao W, Guo J, Ishchenko A, Singh SB, "Design and optimization of renin inhibitors: Orally bioavailable alkyl amines," *Bioorganic & medicinal chemistry letters*, vol. 19, no. 13, pp. 3541-3545, 2009.

[18] Van Der Spoel D, Lindahl E, Hess B, Groenhof G, Mark AE, Berendsen HJC, "GROMACS: fast, flexible, and free," *Journal of computational chemistry*, vol. 26, no. 16, pp. 1701-1718, 2005.

[19] Schuttelkopf AW, Van Aalten DMF, "PRODRG: a tool for high-throughput crystallography of protein-ligand complexes," *Acta Crystallographica Section D: Biological Crystallography*, vol. 60, no. 8, pp. 1355-1363, 2004.

[20] Essmann U, Perera L, Berkowitz ML, Darden T, Lee H, Pedersen LG, "A smooth particle mesh Ewald method," *Journal of Chemical Physics*, vol. 103, no. 19, pp. 8577-8593, 1995.

[21] Hess B, Bekker H, Berendsen HJC, Fraaije JGEM, "LINCS: a linear constraint solver for molecular simulations," *Journal of computational chemistry*, vol. 18, no. 12, pp. 1463-1472, 1997.

[22] Miyamoto S, Kollman PA, "SETTLE: an analytical version of the SHAKE and RATTLE algorithm for rigid water models," *Journal of computational chemistry*, vol. 13, no. 8, pp. 952-962, 1992.

[23] Verdonk ML, Cole JC, Hartshorn MJ, Murray CW, Taylor RD, "Improved protein-ligand docking using GOLD," *Proteins: Structure, Function, and Bioinformatics*, vol. 52, no. 4, pp. 609-623, 2003.